RESEARCH REPORTS
Biological

K. Musselmann[1]*, J.A. Green[1], K. Sone[1], J.C. Hsu[1], I.R. Bothwell[1], S.A. Johnson[1], J.S. Harunaga[1], Z. Wei[2], and K.M. Yamada[1]*

[1]Cell Biology Section, Laboratory of Cell and Developmental Biology, Division of Intramural Research, National Institute of Dental and Craniofacial Research, 30 Convent Drive, MSC 4370, Bethesda, MD 20892, USA; and [2]Developmental Mechanisms Section, Division of Intramural Research, National Institute of Dental and Craniofacial Research, 30 Convent Drive, MSC 4326, Bethesda, MD 20892, USA; *corresponding authors, kurt.musselmann@gmail.com and kenneth.yamada@nih.gov

Salivary Gland Gene Expression Atlas Identifies a New Regulator of Branching Morphogenesis

J Dent Res DOI: 10.1177/0022034511413131

APPENDIX

EXTENDED EXPERIMENTAL PROCEDURES

Salivary Gland Isolation, Tissue Sections, and Laser Microdissection

Embryos from timed-pregnant mice (the morning of the day that the vaginal plug was detected was set to E0) were collected in the mid-afternoon (E12.5 and E13.5) or early morning (E14 and E15), and the salivary glands placed on Nuclepore filters after dissection as previously described (Wei *et al*., 2007). The Nuclepore filters containing explanted SMGs were inverted onto cold OCT (Optimal Cutting Temperature compound at 4°C) in cryosection molds, and the molds were placed on the top of a brass cylinder cooled by ethanol-dry ice. After the OCT was frozen, the filter was carefully removed with forceps, and care was taken to remove the entire filter. The frozen tissue blocks were maintained in the molds at -80°C until being sectioned. A Leica CM3050S research cryostat was used to cut 10- to 14-μm frozen sections, which were collected on PEN membrane glass slides (Applied Biosystems, Carlsbad, CA, USA or Leica, Wetzlar, Germany) pre-treated with 0.01% polylysine for 5 min (Sigma, St. Louis, MO, USA) and then UV-crosslinked for 30 min in a Stratalinker (Stratagene, Santa Clara, CA, USA). The slides were frozen on dry ice and stored at -80°C. Prior to laser capture, the slides were thawed at room temperature for 10 min, stained with 0.1% toluidine blue containing 400 U/mL RNaseOut (Invitrogen, Carlsbad, CA, USA), and air-dried. Laser capture was performed with an Arcturus XT (Applied Biosystems) at the "UV-cut first" (at 15% laser intensity) setting and CapSure HS LCM caps (Applied Biosystems). At least 500 to 1000 cells were collected for each replicate at every location analyzed. The numbers of sections isolated by LCM pooled for each biological replicate are shown in the Table following this section. Cells adjacent to the microdissected areas were also collected by LCM and used to check RNA integrity of the sections by PCR. Three sets of PCR primers for E-cadherin (E-cdh-1, -2, and -3) were designed in MacVector (MacVector Inc., Cary, NC, USA) to generate a 600-bp product 2500, 2000, and 1000 bases upstream of the 3′ end of the mRNA. Laser-captured tissue samples were amplified only if the E-cdh-1 and E-cdh-2 PCR analysis of the adjacent sections showed a band of 600 nt.

Table showing numbers of pooled samples isolated by LCM for each biological replicate:

Location/Age	E12.5	E13.5	E14	E15
Main duct	> 5	> 5	> 5	> 5
Secondary duct		> 10	> 10	> 10
Bud	> 10	PB, > 10; CB, > 10	> 20	> 30
Cleft	> 20	> 20		

Microarray Analysis

Tissue samples collected by LCM were extracted with Buffer RLT (Qiagen, Valencia, CA, USA) or Trizol (Invitrogen) following the manufacturers' protocols. To facilitate RNA precipitation, we added carrier to each sample. For samples extracted in Buffer RLT, 30 ng polyinosine (Sigma-Aldrich, St. Louis, MO, USA) was added; for samples extracted in Trizol, 10 μg Glycoblue (Ambion, Carlsbad, CA, USA) was used. The purified RNA was subjected to 2 rounds of amplification with MessageAMP 2AA (Ambion) following the manufacturers' protocol, with two modifications: The ratio of aminoallyl-UTP:UTP was reduced from 1:1 to 1:3, and the Agilent Spike-In was added to each sample before the second round of amplification. Gene expression in each sample was determined with Whole Mouse Genome arrays (4 x 44k, Agilent, Santa Clara, CA, USA). The images of each array were analyzed with Agilent Feature extraction software 9.3.4 to generate gene expression values and imported into GeneSpring 11.5 (Agilent). They were processed by quantile normalization (Bolstad *et al.,* 2003) and RMA (Irizarry *et al.,* 2003). The imported files were then processed to show genes present in at least 66% of arrays. Comparisons of the expression of 4 housekeeping genes confirmed consistent expression among all of the normalized arrays

(Appendix Fig. 2A). These lists were then subjected to analysis of variance (ANOVA), followed by Tukey's *post hoc* testing to generate lists of genes expressed significantly differently ($P < 0.05$) between each of the individual locations and ages (PM66 AT); the lists have been deposited in GEO as supplemental data along with tables showing the fold-changes of these genes. To validate the microarrays, we collected independent biological replicates (n = at least 3) and amplified them once using the procedure described above, then analyzed them by SYBR-Green qPCR using a StepOnePlus thermal cycler (Applied Biosystems) and calculating ddCT to determine fold change. Primers for qPCR validation were designed with BeaconDesigner (Premier Biosoft International, Palo Alto, CA, USA). The software was instructed to find amplicons within the last 1000 nucleotides of the mRNA, with amplicon lengths 75-200 bases and Tm = 62° ± 2°C. Primers were purchased from Integrated DNA Technologies (IDT), Operon, or the Facility for Biotechnology Resources, CBER, Food and Drug Administration (FDA) and tested for efficiency. Only primers with efficiencies > 85% but < 110% were used in subsequent validation experiments.

GSK3β Inhibitory Studies

E12 SMGs were cultured in medium supplemented with either 20 mM LiCl (Klein and Melton, 1996) or 20 mM NaCl (control) for up to 2 days. The inhibitor SB-216763 (S3442, Sigma-Aldrich; Cross *et al.,* 2001) was used at 10 μM from a 40-mM stock in DMSO. BIO (6-bromoindirubin-3'-oxime; B1686, Sigma-Aldrich; Polychronopoulos *et al*., 2004) was used at 5 μM from a 20-mM stock in DMSO. All samples received a final concentration of 0.025% DMSO. The SMGs were photographed with a Nikon D5000 camera on an Axiovert 40C inverted microscope (Carl Zeiss, Oberkochen, Germany). Clefts from left-and-right pairs of glands (to compare control and experimental conditions using glands from the same mouse) were counted manually, and the data were analyzed for statistical significance with Prism 5 (GraphPad Software, La Jolla, CA, USA) by a one-tailed *t* test. In the LiCl washout (reversal) experiments, SMGs were treated for 16 hrs with LiCl and rinsed twice with fresh DMEM/F12, and culture was continued for 24 hrs.

Image Processing

Photographs were processed in iPhoto (Apple, Cupertino, CA, USA), where color information was discarded, and contrast and levels were adjusted. Immunostaining images acquired with an LSM 710 confocal microscope (Carl Zeiss) were imported into MetaMorph Offline 7.5.6.0 (Molecular Devices, Sunnyvale, CA, USA), where contrast adjustment and a smoothing filter were applied.

Whole-mount and Cryosection Immunofluorescence Microscopy

Whole SMGs were fixed and permeabilized (a) as previously described in 4% paraformaldehyde with 0.1% Triton X-100 permeabilization (Wei *et al*., 2007; Rebustini *et al*., 2009), or (b) in 1:1 acetone:methanol at -20°C for 5 min. The glands were then rinsed 3 times with 0.1% Tween 20/PBS for 15 min each. Non-specific binding sites were then blocked with 5% donkey serum, 1% BSA (Sigma), and M.O.M. (Vector Laboratories, Burlingame, CA, USA) in 0.1% Tween/PBS overnight at 4°C. The glands were then incubated with primary monoclonal antibodies against E-cadherin (ECCD-2, Invitrogen) or GSK3β (Cell Signaling), or with rabbit polyclonal anti-fibronectin antibody R5836 (made in-house) in 0.1% Tween/PBS (containing 8% M.O.M. protein concentrate plus 5% donkey serum) overnight at 4°C. Samples were then incubated with secondary antibodies conjugated to Cy2, Cy3, or Cy5 (Jackson ImmunoResearch Laboratories, West Grove, PA, USA) overnight at 4°C before being mounted on slides. For cryostat sectioning, SMGs were explanted at E12 and cultured until reaching stage E13.5. The glands were fixed with 1:1 acetone:methanol and then frozen in OCT as described for LCM. Cryosections (14 μm) were cut by means of a Leica CM3050S cryostat and collected on positively charged slides. Sections were then treated as described for whole-mount microscopy, except that the incubations were at room temperature for 1 hr. Samples were examined by confocal microscopy (LSM 510 or 710, Carl Zeiss Microimaging).

APPENDIX REFERENCES

Bolstad BM, Irizarry RA, Astrand M, Speed TP (2003). A comparison of normalization methods for high density oligonucleotide array data based on variance and bias. *Bioinformatics* 19:185-193.

Cross DA, Culbert AA, Chalmers KA, Facci L, Skaper SD, Reith AD (2001). Selective small-molecule inhibitors of glycogen synthase kinase-3 activity protect primary neurones from death. *J Neurochem* 77:94-102.

Irizarry RA, Ooi SL, Wu Z, Boeke JD (2003). Use of mixture models in a microarray-based screening procedure for detecting differentially represented yeast mutants. *Stat Appl Genet Mol Biol* 2:Article 1.

Klein PS, Melton DA (1996). A molecular mechanism for the effect of lithium on development. *Proc Natl Acad Sci USA* 93:8455-8459.

Polychronopoulos P, Magiatis P, Skaltsounis AL, Myrianthopoulos V, Mikros E, Tarricone A, *et al.* (2004). Structural basis for the synthesis of indirubins as potent and selective inhibitors of glycogen synthase kinase-3 and cyclin-dependent kinases. *J Med Chem* 47:935-946.

Rebustini IT, Myers C, Lassiter KS, Surmak A, Szabova L, Holmbeck K, *et al.* (2009). MT2-MMP-dependent release of collagen IV NC1 domains regulates submandibular gland branching morphogenesis. *Dev Cell* 17:482-493.

Wei C, Larsen M, Hoffman MP, Yamada KM (2007). Self-organization and branching morphogenesis of primary salivary epithelial cells. *Tissue Eng* 13:721-735.

APPENDIX REFERENCES FOR TABLES 1 AND 2 (MAIN ARTICLE)

1. Hashizume A, Ueno T, Furuse M, Tsukita S, Nakanishi Y, Hieda Y (2004). Expression patterns of claudin family of tight junction membrane proteins in developing mouse submandibular gland. *Dev Dyn* 231:425-431.
2. Jaskoll T, Melnick M (1999). Submandibular gland morphogenesis: stage-specific expression of TGF-alpha/EGF, IGF, TGF-beta, TNF, and IL-6 signal transduction in normal embryonic mice and the phenotypic effects of TGF-beta2, TGF-beta3, and EGF-r null mutations. *Anat Rec* 256:252-268.
3. Kadoya Y, Yamashina S (1993). Distribution of alpha 6 integrin subunit in developing mouse submandibular gland. *J Histochem Cytochem* 41:1707-1714.

4. Geiger S, Geiger B, Leitner O, Marshak G (1987). Cytokeratin polypeptides expression in different epithelial elements of human salivary glands. *Virchows Arch A Pathol Anat Histopathol* 410:403-414.
5. Yamaguchi Y, Yonemura S, Takada S (2006). Grainyhead-related transcription factor is required for duct maturation in the salivary gland and the kidney of the mouse. *Development* 133:4737-4748.
6. Melvin JE, Yule D, Shuttleworth T, Begenisich T (2005). Regulation of fluid and electrolyte secretion in salivary gland acinar cells. *Annu Rev Physiol* 67: 445-469.
7. Thompson-Vest N, Shimizu Y, Hunne B, Furness JB (2006). The distribution of intermediate-conductance, calcium-activated, potassium (IK) channels in epithelial cells. *J Anat* 208:219-229.
8. Begenisich T, Nakamoto T, Ovitt CE, Nehrke K, Brugnara C, Alper SL, *et al.* (2004). Physiological roles of the intermediate conductance, Ca2+-activated potassium channel Kcnn4. *J Biol Chem* 279:47681-47687.
9. Larsen HS, Ruus AK, Galtung HK (2009). Aquaporin expression patterns in the developing mouse salivary gland. *Eur J Oral Sci* 117:655-662.
10. Wei C, Larsen M, Hoffman MP, Yamada KM (2007). Self-organization and branching morphogenesis of primary salivary epithelial cells. *Tissue Eng* 13:721-735.
11. Zeng W, Lee MG, Yan M, Diaz J, Benjamin I, Marino CR, *et al.* (1997). Immuno and functional characterization of CFTR in submandibular and pancreatic acinar and duct cells. *Am J Physiol* 273:C442-C455.
12. Lee MG, Choi JY, Luo X, Strickland E, Thomas PJ, Muallem S (1999). Cystic fibrosis transmembrane conductance regulator regulates luminal Cl-/HCO3- exchange in mouse submandibular and pancreatic ducts. *J Biol Chem* 274:14670-14677.
13. Bult CJ, Eppig JT, Kadin JA, Richardson JE, Blake JA (2008). The Mouse Genome Database (MGD): mouse biology and model systems. *Nucleic Acids Res* 36(Database issue):D724-728.
14. Girard LR, Castle AM, Hand AR, Castle JD, Mirels L (1993). Characterization of common salivary protein 1, a product of rat submandibular, sublingual, and parotid glands. *J Biol Chem* 268:26592-26601.
15. Lombaert IM, Hoffman MP (2010). Epithelial stem/progenitor cells in the embryonic mouse submandibular gland. *Front Oral Biol* 14:90-106.
16. Steinberg Z, Myers C, Heim VM, Lathrop CA, Rebustini IT, Stewart JS *et al*. (2005). FGFR2b signaling regulates ex vivo submandibular gland epithelial cell proliferation and branching morphogenesis. *Development* 132:1223-1234.
17. Knox SM, Hoffman MP (2008). Salivary Gland Development and Regeneration. In: Salivary Diagnostics. D Wong editor. Ames, Iowa: Wiley-Blackwell, p. 13.

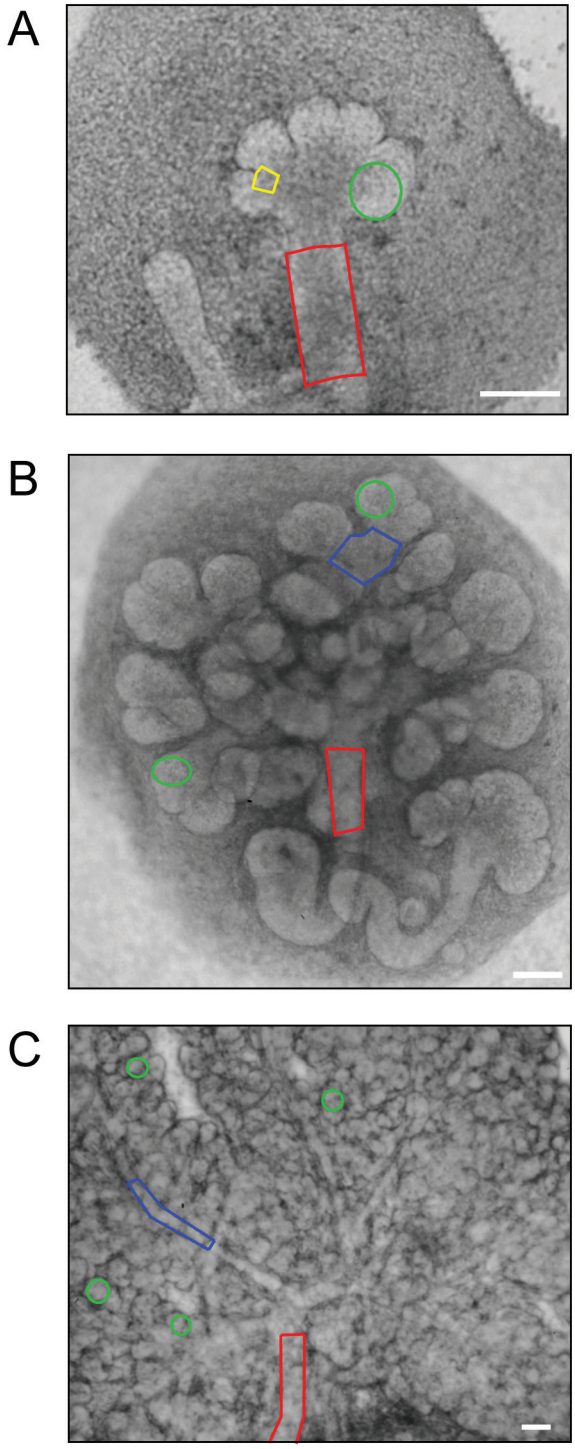

Appendix Figure 1. Representative Images of Submandibular Salivary Glands Indicating Locations Isolated by LCM (A) E12.5, (B) E14, and (C) E15. Color legend: red- main duct; blue- secondary duct; green- bud; yellow- cleft. Scale bar for all images = 100 μm.

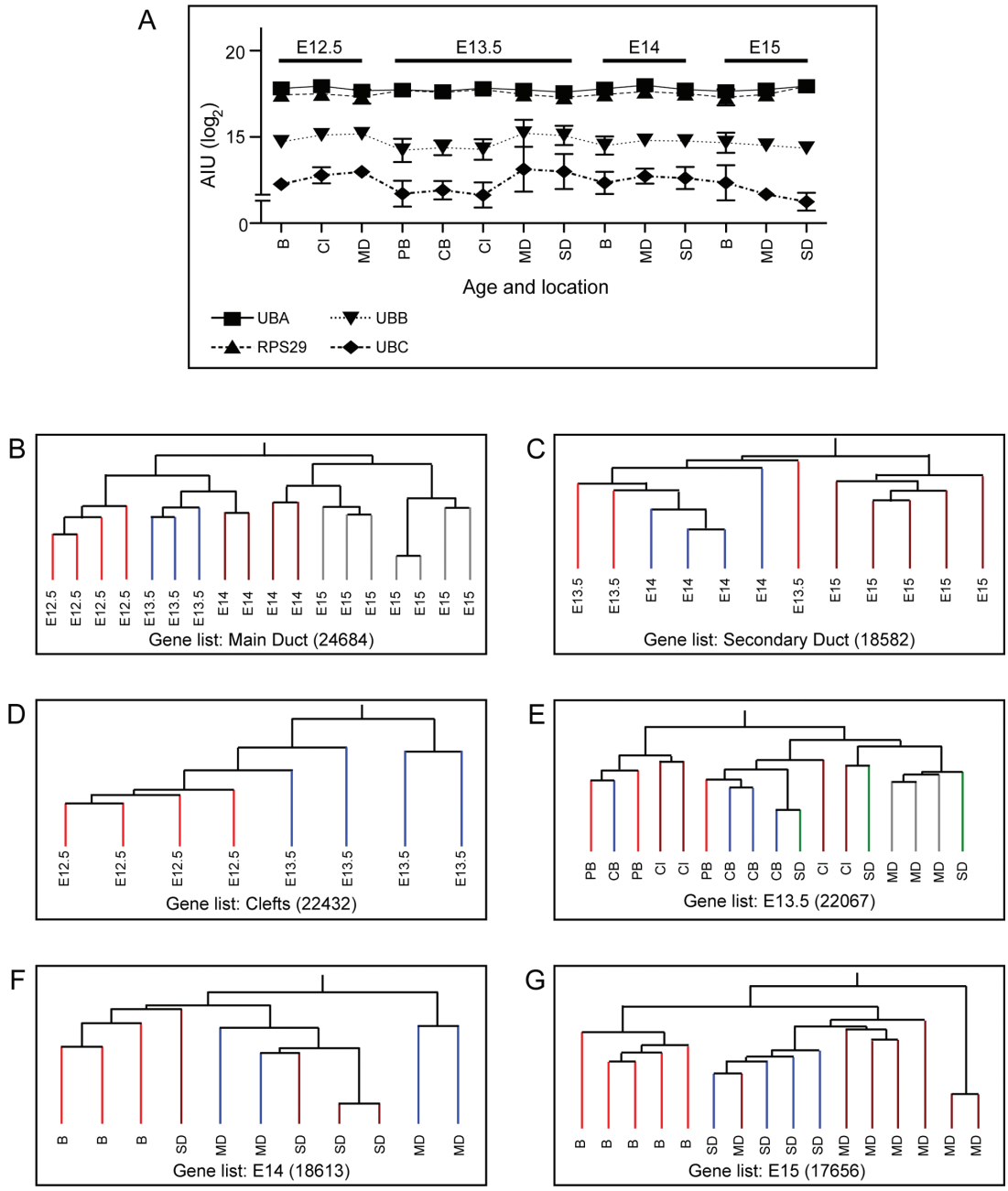

Appendix Figure 2. Results of Normalization and Hierarchical Clustering of Each Location and Age Samples were subjected to hierarchical clustering based on the origin of the biological replicates ("cluster on conditions" analysis based on age or location using GeneSpring). Abbreviations: CB, central bud; Cl, cleft; PB, peripheral bud; MD, main duct; SD, secondary duct. The numbers in parentheses indicate the number of genes present or marginal in at least 66% of the biological replicates at each location. (A) After normalization, the expression of the four housekeeping genes *Rps29, Uba52, Ubb* and *Ubc* was found to be consistent among all of the normalized arrays (Figure 2A). The data are now available on the website http://sgmap.nidcr.nih.gov/ in a searchable format and in GEO (Accession number GSE22828). (B-G) Clustering analysis showed that all arrays were nested, and the biological replicates clustered together compared to biological replicates at other locations. (B) Clustering of main duct arrays (24684 genes present or marginal). The E12.5 and E13.5 main duct arrays and some of the E14 arrays were nested, suggesting that gene expression in these arrays was similar. A separate nested group contained the remaining E14 arrays and all of the E15 arrays. Within the subclusters, the arrays clustered according to age. (C) Clustering of secondary duct arrays (18582 genes present or marginal). The E13.5 and E14 secondary duct arrays were nested and formed a subcluster indicating similar gene expression patterns. The E15 secondary duct arrays formed a distinct subcluster. (D) Clustering of cleft arrays (22432 genes present or marginal). The biological replicates clustered according to age. (E) Clustering of E13.5 arrays (22067 genes present or marginal). The peripheral and central bud arrays formed a nested cluster, indicating that gene expression in these arrays was very similar. The cleft arrays did not form a single distinct subcluster. The main duct arrays clustered together, but the secondary duct arrays did not. (F) Clustering of E14 arrays (18613 genes present or marginal). Main ducts and secondary ducts are nested, suggesting similarity in gene expression, but they are different from bud arrays. (G) Clustering of E15 arrays (17656 genes present or marginal). The bud arrays clustered together and are different from the main and secondary duct arrays, which are nested, suggesting similar gene expression profiles for ducts.

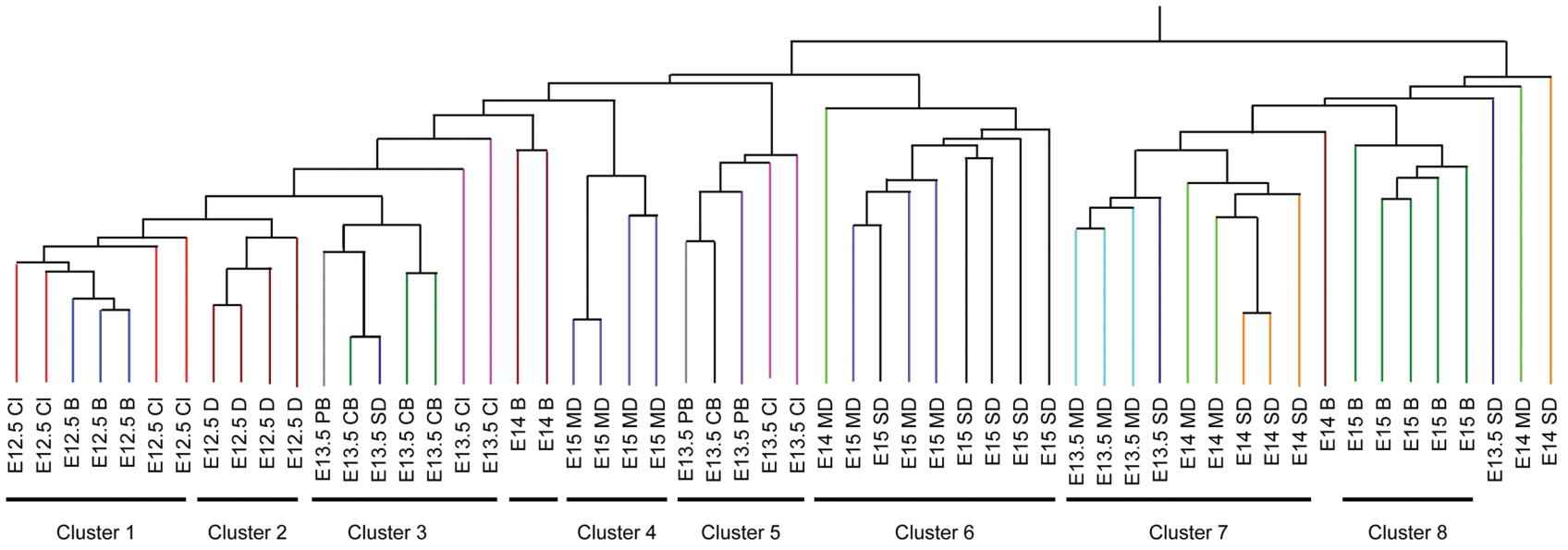

Appendix Figure 3. Hierarchical Cluster of All Arrays The complete dataset was subjected to hierarchical clustering on condition (age or location using GeneSpring) and the arrays clustered into 8 clusters. The E12.5 bud and cleft arrays clustered together, as did the E12.5 main duct arrays. The arrays from the E13.5 endbud structures (peripheral and central bud, and clefts) clustered together, as did the early ducts (E13.5 main duct and E14 main and secondary ducts). The late ducts formed two clusters (one E15 main duct group and a group containing the E15 main and secondary ducts). The E14 bud arrays did not all cluster together, and two clustered closer to E13.5 cleft arrays. Three of the duct arrays (E13.5 secondary duct, E14 main and secondary duct) did not cluster.

Appendix Table 1. Bioinformatics Comparison of E15 Bud to E15 Main Duct

Molecular Function Gene Ontology			Up in E15 Bud Compared with E15 Main Duct		
Term	Count	*P*-value	Fold Enrichment	Q-value	Genes
GO:0016209~anti-oxidant activity	4	0.02	7.42	0.95	GPX2, GSR, LPO, TXNRD2
GO:0008047~enzyme activator activity	9	0.02	2.68	0.90	ARHGDIG, RGS11, ACAP3, RAP1GAP, PLEKHG6, 1190002H23RIK, GPSM3, SEC14L2, MGST2
GO:0003924~GTPase activity	6	0.03	3.48	0.93	GFM2, TUBA-RS1, EFTUD2, TUBA3A, EIF5B, GNG2
GO:0030145~manganese ion binding	6	0.05	3.01	0.97	GALNT3, PPM1D, PHLPP2, PPM1K, ENDOG, GALNT12
Molecular Function Gene Ontology			Down in E15 Bud Compared with E15 Main Duct		
Term	Count	*P*-value	Fold Enrichment	Q-value	Genes
GO:0046983~protein dimerization activity	11	0.00	3.14	0.33	CHKA, IKZF2, CCDC88A, EPAS1, ADH1, JUN, RUNX1T1, CREB5, PBX1, ZFP618, TGFB2
GO:0008092~cytoskeletal protein binding	12	0.00	2.81	0.23	RAB11FIP5, TRIM2, KIF1B, CCDC88A, CLMN, CEP290, CLIP1, SCNN1A, ADD3, VILL, PLS3, APC
GO:0043167~ion binding	54	0.01	1.33	0.51	ATP1B1, PSTK, VILL, CNOT4, TRIM2, P4HA2, CAT, GM5595, AGAP1, NT5E, PLS3, ZCCHC7, RREB1, RUNX1T1, CFTR, COLEC12, CDO1, THBD, CLIC6, 2810408P10RIK, CLIP1, PGCP, LRRK1, ADD3, NSD1, TRIM39, ALOX12, PHYHD1, TSHZ3, CLCN2, PPP2R3A, CYP2F2, ZFP618, ADH1, CASZ1, SLC4A7, PLCD1, SCNN1A, ZBTB7C, IKZF2, L3MBTL2, CREB5, PCDH17, MANBA, ITPR2, NOTCH2, JHDM1D, CDKN1A, PRICKLE1, SULF2, FBLN5, PLCG2, MPPED2, GPATCH8
GO:0030528~transcription regulator activity	21	0.02	1.69	0.66	TSHZ3, IKZF2, EPAS1, MAFB, RUNX1T1, TEAD1, CREB5, DACH1, PPARGC1A, PPARGC1B, TCFCP2L1, MYCL1, MEIS2, JUN, NFAT5, CEP290, PBX1, RUNX1, LCOR, NSD1, RUNX2
GO:0003700~transcription factor activity	15	0.03	1.87	0.70	TSHZ3, EPAS1, MAFB, RUNX1T1, TEAD1, CREB5, DACH1, MYCL1, MEIS2, JUN, NFAT5, PBX1, RUNX1, LCOR, RUNX2
GO:0016702~oxidoreductase activity, acting on single donors with incorporation of molecular oxygen, incorporation of 2 atoms of oxygen	4	0.03	5.71	0.71	PHYHD1, P4HA2, CDO1, ALOX12
GO:0043169~cation binding	51	0.03	1.27	0.65	ATP1B1, PSTK, VILL, CNOT4, TRIM2, P4HA2, CAT, GM5595, AGAP1, NT5E, PLS3, ZCCHC7, RREB1, RUNX1T1, COLEC12, CDO1, THBD, 2810408P10RIK, CLIP1, PGCP, ADD3, NSD1, LRRK1, TRIM39, ALOX12, PHYHD1, TSHZ3, PPP2R3A, CYP2F2, ZFP618, ADH1, CASZ1, SLC4A7, PLCD1, SCNN1A, ZBTB7C, IKZF2, L3MBTL2, CREB5, PCDH17, MANBA, ITPR2, NOTCH2, JHDM1D, CDKN1A, SULF2, PRICKLE1, FBLN5, PLCG2, MPPED2, GPATCH8
GO:0019838~growth factor binding	4	0.04	5.39	0.65	IGF1R, IL1RL2, PDGFRA, CYR61
GO:0015293~symporter activity	5	0.05	3.67	0.67	SLC16A2, SLC6A9, SLC16A11, SLC6A6, SLC4A7
GO:0042803~protein homodimerization activity	6	0.05	3.02	0.66	CHKA, IKZF2, CCDC88A, ADH1, RUNX1T1, TGFB2
KEGG Pathways			Up in E15 Bud Compared with E15 Main Duct		
Term	Count	*P*-value	Fold Enrichment	Q-value	Genes
mmu03040:Spliceosome	6	0.02	3.65	0.75	BCAS2, PPIH, EFTUD2, SNRPB, LSM2, SF3B5

(continued)

Appendix Table 1. (continued)

KEGG Pathways					Down in E15 Bud Compared with E15 Main Duct
Term	Count	*P*-value	Fold Enrichment	Q-value	Genes
mmu05210:Colorectal cancer	7	0.00	7.78	0.01	IGF1R, FZD10, JUN, PDGFRA, AXIN2, APC, TGFB2
mmu04310:Wnt signaling pathway	8	0.00	5.13	0.02	CSNK1A1, WNT10A, FZD10, PRICKLE1, JUN, NFAT5, AXIN2, APC
mmu05217:Basal cell carcinoma	4	0.02	6.96	0.36	WNT10A, FZD10, AXIN2, APC
mmu05214:Glioma	4	0.03	5.98	0.41	IGF1R, CDKN1A, PLCG2, PDGFRA
mmu04070:Phosphatidylinositol signaling system	4	0.04	5.10	0.48	INPP5K, PLCG2, PLCD1, ITPR2

We generated gene lists by identifying genes whose expression differed 5-fold or higher among the bud, main duct, and secondary duct of E15 salivary glands. These lists were analyzed by DAVID (Database for Annotation, Visualization and Integrated Discovery) to identify overrepresented pathways and molecular function gene ontology terms. *P*-values for each group of genes were calculated by DAVID with a modified Fisher's Exact test (EASE-score). Fold enrichment numbers were calculated as the ratio of the percentage of the genes belonging to the pathway in the gene list compared with the percentage expected by chance alone, and the Benjamini-Hochberg procedure was used to determine the false discovery rate (Q-value).

Appendix Table 2. Bioinformatics Comparison of E15 Bud to E15 Secondary Duct

Molecular Function Gene Ontology	Up in E15 Bud Compared with E15 Secondary Duct				
Term	Count	*P*-value	Fold Enrichment	Q-value	Genes
GO:0008047~enzyme activator activity	7	0.00	4.79	0.45	ARHGDIG, RALGAPA1, CAV1, RGS2, RAP1GAP, 1190002H23RIK, GPSM3
GO:0005509~calcium ion binding	11	0.02	2.23	0.88	ITGA6, GALNT7, PLS1, PADI2, DLK1, GALNT12, PROS1, CANX, GAS6, MYL9, PCDH18
GO:0030528~transcription regulator activity	13	0.04	1.84	0.88	SOX7, CITED1, MAPK1, HEY1, BHLHA15, GTF2A2, TEAD4, SPDEF, FABP4, ETV1, ID4, CREB3L4, MYB
Molecular Function Gene Ontology	Down in E15 Bud Compared with E15 Secondary Duct				
Term	Count	*P*-value	Fold Enrichment	Q-value	Genes
GO:0043167~ion binding	37	0.01	1.44	0.92	TSHZ3, ATP1B1, CLCN2, LTBP2, CYP2F2, ADCY8, LTBP4, VILL, CD97, TRIM2, P4HA2, ADH1, LTF, ZFP521, GM5595, NT5E, RASA2, IKZF2, ZBTB7C, CFTR, CDO1, MANBA, MMP11, ITPR2, CDKN1A, THBD, PRICKLE1, SULF2, FBLN5, CLIC6, PLCG2, MPPED2, LIME1, PGCP, LRRK1, ADAM15, ALOX12
GO:0015293~symporter activity	5	0.01	5.79	0.73	SLC16A2, SLC6A9, SLC22A18, SLC16A11, SLC6A6
GO:0070011~peptidase activity, acting on L-amino acid peptides	9	0.04	2.28	0.97	TMPRSS2, KLK1B8, PGPEP1, PSEN1, LTF, HP, PGCP, ADAM15, MMP11
GO:0005160~transforming growth factor beta receptor binding	2	0.04	43.64	0.89	TGFB3, TGFB2
KEGG Pathways	Up in E15 Bud Compared with E15 Secondary Duct				
Term	Count	*P*-value	Fold Enrichment	Q-value	Genes
mmu04510:Focal adhesion	5	0.04	3.62	0.98	MAPK1, LAMA4, CAV1, ITGA6, MYL9
mmu00480:Glutathione metabolism	3	0.05	8.28	0.90	LAP3, GPX2, GGCT
KEGG Pathways	Down in E15 Bud Compared with E15 Secondary Duct				
Term	Count	*P*-value	Fold Enrichment	Q-value	Genes
mmu05200:Pathways in cancer	9	0.00	4.10	0.08	WNT10A, CDKN1A, EPAS1, SOS1, JUN, PLCG2, TGFB3, AXIN2, TGFB2
mmu05211:Renal cell carcinoma	5	0.00	10.51	0.04	EPAS1, SOS1, JUN, TGFB3, TGFB2
mmu05210:Colorectal cancer	5	0.00	8.55	0.06	SOS1, JUN, TGFB3, AXIN2, TGFB2
mmu04020:Calcium signaling pathway	6	0.01	4.62	0.15	PHKA2, EDNRA, ADCY8, PLCG2, ITPKA, ITPR2
mmu04310:Wnt signaling pathway	5	0.02	4.94	0.20	WNT10A, PSEN1, PRICKLE1, JUN, AXIN2
mmu04012:ErbB signaling pathway	4	0.02	6.76	0.20	CDKN1A, SOS1, JUN, PLCG2
mmu04912:GnRH signaling pathway	4	0.03	6.07	0.23	ADCY8, SOS1, JUN, ITPR2

We generated gene lists by identifying genes whose expression differed 5-fold or higher among the bud, main duct, and secondary duct of E15 salivary glands. These lists were analyzed by DAVID (Database for Annotation, Visualization and Integrated Discovery) to identify overrepresented pathways and molecular function gene ontology terms. *P*-values for each group of genes were calculated by DAVID with a modified Fisher's Exact test (EASE-score). Fold enrichment numbers were calculated as the ratio of the percentage of the genes belonging to the pathway in the gene list compared with the percentage expected by chance alone, and the Benjamini-Hochberg procedure was used to determine the false discovery rate (Q-value).

Appendix Table 3. Bioinformatics Comparison of E15 Main Duct to E15 Secondary Duct

Molecular Function Gene Ontology	Up in E15 Main Duct Compared with E15 Secondary Duct				
Term	Count	*P*-value	Fold Enrichment	Q-value	Genes
GO:0008017~microtubule binding	4	0.00	17.09	0.16	KIF1B, CCDC88A, CEP290, CLIP1
GO:0008092~cytoskeletal protein binding	7	0.00	4.41	0.16	MTSS1, KIF1B, CCDC88A, LIMCH1, CEP290, CLIP1, SYNPO
GO:0030528~transcription regulator activity	12	0.00	2.59	0.12	TAF7, ZFP449, RUNX1T1, CEP290, FABP4, CREB5, PBX1, ZEB2, SOX7, LCOR, FOXN3, TCFCP2L1
GO:0003700~transcription factor activity	8	0.03	2.69	0.44	ZFP449, RUNX1T1, CREB5, PBX1, ZEB2, SOX7, LCOR, FOXN3
GO:0046983~protein dimerization activity	5	0.04	3.83	0.53	CCDC88A, RUNX1T1, CREB5, PBX1, TERF2
GO:0016564~transcription repressor activity	4	0.04	4.94	0.53	RUNX1T1, FABP4, ZEB2, TCFCP2L1
Molecular Function Gene Ontology	Down in E15 Main Duct Compared with E15 Secondary Duct				
Term	Count	*P*-value	Fold Enrichment	Q-value	Genes
GO:0046872~metal ion binding	28	0.00	1.61	0.57	ADAMTS18, PHLPP2, MYL10, DMPK, PCDH1, MAP3K4, ANG, FXC1, ZFP296, EFCAB2, ENTPD4, MT4, ZFYVE1, SLC12A8, ADARB1, CRIP3, GDE1, ZMYM6, ATP1A3, IDO2, ACLY, ZFP606, MID1, CACNA2D3, PTHLH, PITPNM2, RNF6, ZNHIT1
GO:0019208~phosphatase regulator activity	3	0.01	16.61	0.48	SBF2, PPP2R5A, PPP2R5C
GO:0005543~phospholipid binding	4	0.02	7.44	0.45	PITPNM2, SBF2, ZFYVE1, SNX11
GO:0000287~magnesium ion binding	6	0.03	3.25	0.67	MAP3K4, GDE1, ATP1A3, ACLY, ENTPD4, DMPK
KEGG Pathway	Up in E15 Main Duct Compared with E15 Secondary Duct				
None					
KEGG Pathway	Down in E15 Main Duct Compared with E15 Secondary Duct				
Term	Count	*P*-value	Fold Enrichment	Q-value	Genes
mmu05211:Renal cell carcinoma	3	0.03	11.18	0.82	PGF, SOS1, GAB1

We generated gene lists by identifying genes whose expression differed 5-fold or higher among the bud, main duct, and secondary duct of E15 salivary glands. These lists were analyzed by DAVID (Database for Annotation, Visualization and Integrated Discovery) to identify overrepresented pathways and molecular function gene ontology terms. *P*-values for each group of genes were calculated by DAVID with a modified Fisher's Exact test (EASE-score). Fold enrichment numbers were calculated as the ratio of the percentage of the genes belonging to the pathway in the gene list compared with the percentage expected by chance alone, and the Benjamini-Hochberg procedure was used to determine the false discovery rate (Q-value).

Appendix Table 4. Molecular Function Analysis of Genes Used for qPCR Validation

Molecular Function Gene Ontology		Genes from Literature Used for qPCR Validation
Term	Count	Genes
GO:0005198~structural molecule activity	9	KRT19, KRT18, KRT17, CLDN4, CLDN3, CLDN6, KRT7, KRT8, CLDN11
GO:0042802~identical protein binding	4	CLDN4, CLDN3, CLDN6, CLDN11
GO:0022838~substrate specific channel activity	4	AQP5, CFTR, SCNN1B, SCNN1A
GO:0015267~channel activity	4	AQP5, CFTR, SCNN1B, SCNN1A
GO:0022803~passive transmembrane transporter activity	4	AQP5, CFTR, SCNN1B, SCNN1A
GO:0050699~WW domain binding	2	SCNN1B, SCNN1A
GO:0019903~protein phosphatase binding	2	CDH1, CTNNB1
GO:0019902~phosphatase binding	2	CDH1, CTNNB1
GO:0005272~sodium channel activity	2	SCNN1B, SCNN1A
GO:0005216~ion channel activity	3	CFTR, SCNN1B, SCNN1A

Appendix Table 5. Embryonic Day 15 Bud *vs.* Embryonic Day 12.5 Bud, Selected Functions, and Pathways of Genes Differentially Expressed

Gene Symbol	Fold Change in Microarray	Fold Change by qPCR	References with Localization Data
Substrate specific transport			
Kcnn4	10.9	6.5	**IF: late bud**; Appendix Ref. 6, 7, 8
Aqp5	1219	38	**qPCR: late bud**; Appendix Ref. 9, 10
Transcription activator activity			
Rnf6	117	–	–
Nfix	26.1	–	–
Cited2	17.3	–	–
Cited4	20.7	–	–
Lef1	–52	–	–
Foxc2	–20	–	–
Smad3	-16.5	–	–
Etv4	–4.5	–	**qPCR: E13 bud**; Appendix Ref. 15
Etv5	–6	–	**qPCR: E13 bud**; Appendix Ref. 15
Enzyme inhibitory activity/peptidase inhibitor activity			
Wfdc3	59.1	–	–
Bc048546	31.1	–	–
Expi	176.5	–	–
Ppp1R1b	18.9	–	–
Serpinb12	43	–	–
Tesc	80.8	–	–
Metallopeptidase activity			
Mmp2	–359.0	–110	**qPCR: E13 SMG**; Appendix Ref. 16
Adamts19	–22.5	–	–
Adamts4	–15.8	–	–
Adamts8	–51.9	–	–
No function assigned			
Dcpp1	3477	d	**ISH: E14.5**; Appendix Ref. 13, 14
Pip	150	11	**qPCR: E15 SMG**; Appendix Ref. 10
Smgc	444	d	**qPCR: E15 SMG**; Appendix Ref. 17
Heme binding			
Hba-A1	38.8	–	–
Hbb-B1	55.2	–	–
Cyp4B1	99.6	–	–
Cyp51	48.8	–	–
Lpo	19.4	–	–
KEGG: Pathways in cancer			
Fgfr2	–15	–3.5	**IF: E13 SMG**; Appendix Ref. 16
Wnt10a	–17	–	–
E2F2	18	–	–
Map2k1	–22.6	–	–
Rxra	–12.2	–	–
Smad3	–16.5	–	–
Lef1	–52	–	–
Mmp2	–359	–110	**qPCR: E13 SMG**; Appendix Ref. 16

For abbreviations, please refer to Table 1 (main article).

Appendix Table 6. Bioinformatics Comparison of E15 Bud to E12.5 Bud

Molecular Function Gene Ontology	Up in E12.5 Bud Compared with E15 Bud				
Term	Count	*P*-value	Fold Enrichment	Q-value	Genes
GO:0008237~metallopeptidase activity	10	0.01	2.81	0.97	ADAMTS9, ADAMTS19, ADAMTS8, COPS5, THSD4, CPXM2, ADAMTS3, MMP2, ADAMTS4, CPZ
GO:0046914~transition metal ion binding	66	0.01	1.33	0.83	GM6685, PXDN, COPS5, BC027344, ZFP334, UTRN, RNF214, ZNRF1, MMP2, ZFP786, RBM4B, ZFP91, RNF219, TIMM9, RARB, 6330439K17RIK, CPXM2, ZHX3, UBR1, MBNL1, GALNTL1, 5730601F06RIK, NUDT11, ZFP592, NEBL, ADAMTS9, ADAMTS8, PPM1K, ZDHHC13, ACAP2, ADAMTS3, STEAP1, TRIM39, ADAMTS4, CYP1B1, ADAMTS19, AKAP13, MYO9A, CPZ, TRIM11, ZFP317, RNF160, ZFP451, ZFP192, RASGRP1, RNFT2, SLC39A8, SLC30A9, LOC100045359, GALNT14, SCO1, ZC3H12C, DNMT3A, ZFP386, FADS1, SMG1, TRIM25, ZFP2, ZFP606, ISL1, RIMKLA, CDKN1A, RNF150, ZFP182, ZFP773, ZMYND17
GO:0016563~transcription activator activity	12	0.01	2.43	0.73	KAT2B, COPS5, CAMK4, LEF1, ATP6V0A1, FOXC2, SMAD3, TBX1, POU3F1, MED13, RBM39, RARB
GO:0008270~zinc ion binding	54	0.02	1.35	0.78	COPS5, BC027344, ZFP334, UTRN, ZNRF1, RNF214, MMP2, ZFP786, ZFP91, RBM4B, RNF219, TIMM9, RARB, 6330439K17RIK, CPXM2, ZHX3, 5730601F06RIK, MBNL1, UBR1, ZFP592, NEBL, ADAMTS9, ADAMTS8, ZDHHC13, ACAP2, ADAMTS3, TRIM39, ADAMTS4, ADAMTS19, AKAP13, MYO9A, CPZ, TRIM11, ZFP317, ZFP451, RNF160, ZFP192, RASGRP1, RNFT2, SLC39A8, SLC30A9, LOC100045359, ZC3H12C, DNMT3A, ZFP386, TRIM25, ZFP2, ISL1, ZFP606, CDKN1A, RNF150, ZFP182, ZFP773, ZMYND17
GO:0004222~metalloendopeptidase activity	7	0.02	3.23	0.79	ADAMTS9, ADAMTS19, ADAMTS8, THSD4, ADAMTS3, MMP2, ADAMTS4
GO:0003682~chromatin binding	8	0.03	2.71	0.83	CHD9, DNMT3A, ZFP386, LEF1, ATP6V0A1, FOXC2, ISL1, PITX2
GO:0046872~metal ion binding	88	0.03	1.20	0.80	PXDN, GM6685, LTBP1, COPS5, BC027344, NPNT, ZFP334, UTRN, NCS1, RNF214, ZNRF1, MMP2, ZFP786, RBM4B, ZFP91, RNF219, TIMM9, RARB, TRPV6, SLC12A7, 6330439K17RIK, REV1, SCN2B, PFKP, ZHX3, CPXM2, PCDH8, UBR1, MBNL1, GALNTL1, NUDT11, 5730601F06RIK, ZFP592, NEBL, ADAMTS9, ADAMTS8, CAMK4, PPM1K, ZDHHC13, ACAP2, FKBP14, ADAMTS3, STEAP1, ADD3, TRIM39, ADAMTS4, CYP1B1, ADAMTS19, AKAP13, MYO9A, TRIM11, ZFP317, CPZ, RNF160, ZFP451, FGG, ZFP192, RASGRP1, DNER, RNFT2, SLC39A8, CERK, SLC30A9, ZC3H12C, LOC100045359, GALNT14, SCO1, DNMT3A, KCNB1, ZFP386, FADS1, MRC2, SMG1, TRIM25, ZFP2, ITGA4, ZFP606, ATP13A3, ISL1, RIMKLA, CDKN1A, LRP1, RNF150, ZFP182, ZFP773, HPCA, LRP8, ZMYND17
GO:0043169~cation binding	88	0.04	1.19	0.83	PXDN, GM6685, LTBP1, COPS5, BC027344, NPNT, ZFP334, UTRN, NCS1, RNF214, ZNRF1, MMP2, ZFP786, RBM4B, ZFP91, RNF219, TIMM9, RARB, TRPV6, SLC12A7, 6330439K17RIK, REV1, SCN2B, PFKP, ZHX3, CPXM2, PCDH8, UBR1, MBNL1, GALNTL1, NUDT11, 5730601F06RIK, ZFP592, NEBL, ADAMTS9, ADAMTS8, CAMK4, PPM1K, ZDHHC13, ACAP2, FKBP14, ADAMTS3, STEAP1, ADD3, TRIM39, ADAMTS4, CYP1B1, ADAMTS19, AKAP13, MYO9A, TRIM11, ZFP317, CPZ, RNF160, ZFP451, FGG, ZFP192, RASGRP1, DNER, RNFT2, SLC39A8, CERK, SLC30A9, ZC3H12C, LOC100045359, GALNT14, SCO1, DNMT3A, KCNB1, ZFP386, FADS1, MRC2, SMG1, TRIM25, ZFP2, ITGA4, ZFP606, ATP13A3, ISL1, RIMKLA, CDKN1A, LRP1, RNF150, ZFP182, ZFP773, HPCA, LRP8, ZMYND17

(continued)

Appendix Table 6. (continued)

GO:0019208~phosphatase regulator activity	4	0.04	5.25	0.81	PHACTR1, SBF2, PPP2R2B, IGFBP3
GO:0030695~GTPase regulator activity	13	0.04	1.89	0.79	ARHGEF3, RALGPS2, SIPA1L2, ARHGEF17, AKAP13, DGKI, MYO9A, ARHGAP25, PLEKHG1, KRIT1, RASGRP1, ACAP2, LOC100045359
GO:0060589~nucleoside-triphosphatase regulator activity	13	0.05	1.86	0.80	ARHGEF3, RALGPS2, SIPA1L2, ARHGEF17, AKAP13, DGKI, MYO9A, ARHGAP25, PLEKHG1, KRIT1, RASGRP1, ACAP2, LOC100045359
GO:0008134~transcription factor binding	11	0.05	2.01	0.78	KAT2B, COPS5, DIP2C, ATP6V0A1, TRIB3, SMAD3, SKI, MED13, RBM39, NRIP1, PITX2
GO:0030528~transcription regulator activity	32	0.05	1.39	0.76	COPS5, E2F6, TRIB3, TAL2, MYCL1, POU5F2, ZFP192, RARB, POU3F1, SCX, PITX2, RHOX5, KAT2B, SSBP2, ZFP386, ARID3A, ZHX3, LEF1, SMAD3, TBX1, SKI, MED13, ISL1, FOXN3, NRIP1, GCFC1, CAMK4, CSRNP2, IRF8, ATP6V0A1, FOXC2, RBM39
GO:0043167~ion binding	88	0.05	1.17	0.74	PXDN, GM6685, LTBP1, COPS5, BC027344, NPNT, ZFP334, UTRN, NCS1, RNF214, ZNRF1, MMP2, ZFP786, RBM4B, ZFP91, RNF219, TIMM9, RARB, TRPV6, SLC12A7, 6330439K17RIK, REV1, SCN2B, PFKP, ZHX3, CPXM2, PCDH8, UBR1, MBNL1, GALNTL1, NUDT11, 5730601F06RIK, ZFP592, NEBL, ADAMTS9, ADAMTS8, CAMK4, PPM1K, ZDHHC13, ACAP2, FKBP14, ADAMTS3, STEAP1, ADD3, TRIM39, ADAMTS4, CYP1B1, ADAMTS19, AKAP13, MYO9A, TRIM11, ZFP317, CPZ, RNF160, ZFP451, FGG, ZFP192, RASGRP1, DNER, RNFT2, SLC39A8, CERK, SLC30A9, ZC3H12C, LOC100045359, GALNT14, SCO1, DNMT3A, KCNB1, ZFP386, FADS1, MRC2, SMG1, TRIM25, ZFP2, ITGA4, ZFP606, ATP13A3, ISL1, RIMKLA, CDKN1A, LRP1, RNF150, ZFP182, ZFP773, HPCA, LRP8, ZMYND17
GO:0019902~phosphatase binding	3	0.05	7.88	0.74	SBF2, SAPS3, DLG1
GO:0008373~sialyltransferase activity	3	0.05	7.88	0.74	ST6GALNAC6, ST6GALNAC3, ST8SIA2
GO:0003712~transcription cofactor activity	8	0.06	2.33	0.73	KAT2B, COPS5, ATP6V0A1, TRIB3, SKI, MED13, RBM39, NRIP1
GO:0043566~structure-specific DNA binding	5	0.06	3.46	0.71	SSBP2, SSBP1, FOXC2, SMAD3, HNRNPA1
GO:0005343~organic acid:sodium symporter activity	3	0.06	7.16	0.74	SLC6A9, SLC1A6, SLC6A13
GO:0015171~amino acid transmembrane transporter activity	4	0.07	4.20	0.75	SLC6A9, SLC7A3, SLC1A6, SLC6A13
GO:0034481~chondroitin sulfotransferase activity	2	0.07	26.26	0.75	CHST11, CHST3
GO:0004190~aspartic-type endopeptidase activity	3	0.09	5.84	0.81	DDI2, NRIP3, H13
GO:0070001~aspartic-type peptidase activity	3	0.09	5.84	0.81	DDI2, NRIP3, H13
GO:0004601~peroxidase activity	3	0.10	5.63	0.82	PXDN, PRDX6, PRDX4
GO:0016684~oxidoreductase activity, acting on peroxide as acceptor	3	0.10	5.63	0.82	PXDN, PRDX6, PRDX4

(continued)

Appendix Table 6. (continued)

Molecular Function Gene Ontology			Down in E12.5 Bud Compared with E15 Bud		
Term	Count	*P*-value	Fold Enrichment	Q-value	Genes
GO:0016563~transcription activator activity	19	0.00	2.34	0.50	MEF2A, KAT2B, COPS5, NR4A2, SMAD3, LEF1, NFIX, TBX1, MED13, CITED4, CITED2, RNF6, CAMK4, ATP6V0A1, FOXC2, RARB, RBM39, POU3F1, NFIC
GO:0019208~phosphatase regulator activity	6	0.01	4.79	0.87	PHACTR1, TESC, PPP1R1B, SBF2, PPP2R2B, IGFBP3
GO:0030528~transcription regulator activity	53	0.01	1.40	0.84	E2F2, MEF2A, COPS5, E2F6, PRRX1, RORC, CITED4, CITED1, CITED2, POU5F2, BHLHA15, HEY2, CREB3L4, RARB, NRG1, SCX, PITX2, SSBP2, ZHX3, LEF1, MED13, DMRTB1, FOXN3, NRIP1, ELL2, CAMK4, SPDEF, FOXC2, RBM39, TRIB3, NFIX, NR3C1, TAL2, MYCL1, TCEA3, ZFP192, POU3F1, KAT2B, RHOX5, ZFP386, NR4A2, ARID3A, SMAD3, SKI, TBX1, ISL1, GCFC1, RNF6, CSRNP2, IRF8, FABP4, ATP6V0A1, NFIC
GO:0008373~sialyltransferase activity	4	0.02	6.39	0.95	ST6GALNAC6, ST6GALNAC3, ST8SIA6, ST8SIA2
GO:0019841~retinol binding	3	0.02	11.98	0.92	RBP4, RBP7, RBP1
GO:0019888~protein phosphatase regulator activity	5	0.03	4.32	0.91	PHACTR1, TESC, PPP1R1B, PPP2R2B, IGFBP3
GO:0016918~retinal binding	3	0.03	10.65	0.90	RBP4, RBP7, RBP1
GO:0032403~protein complex binding	7	0.03	2.87	0.90	GRB10, LYN, LGALS3, NPNT, ITGB1, ADORA1, PIK3R1
GO:0020037~heme binding	10	0.04	2.22	0.89	HBA-A1, CYP51, HBA-A2, GM6685, LPO, PXDN, CYP1B1, CYP2F2, FADS1, HBB-B1, CYP4B1
GO:0030246~carbohydrate binding	17	0.04	1.71	0.89	LY75, LMAN1L, LGALS3, FGF9, MRC2, PGLYRP1, PF4, GALNTL1, VIT, GPCPD1, A930038C07RIK, ADAMTS8, EGFLAM, CLEC2D, APOH, 2900064A13RIK, GALNT14
GO:0008289~lipid binding	18	0.04	1.67	0.88	BC018465, RBP4, RBP7, RBP1, FFAR2, NR3C1, SEC14L4, MYO9A, ACBD3, PEX1, SBF2, RASGRP1, PSP, APOH, FABP4, SNX24, SNX10, HIP1
GO:0046906~tetrapyrrole binding	10	0.05	2.12	0.88	HBA-A1, CYP51, HBA-A2, GM6685, LPO, PXDN, CYP1B1, CYP2F2, FADS1, HBB-B1, CYP4B1
GO:0005372~water transporter activity	3	0.05	7.99	0.89	AQP5, SLC14A1, AQP3
GO:0046914~transition metal ion binding	96	0.05	1.18	0.87	MOCOS, GM6685, BC027344, UTRN, ZFP334, RBM5, RORC, ZNRF1, RNF214, MMP2, ZFP786, ISG20, ZFP91, RNF219, TIMM9, HBB-B1, RARB, DDAH1, 6330439K17RIK, PDXK, ZHX3, NUDT11, UBR1, NEBL, ZFP592, ADAMTS9, ADAMTS8, ACAP2, ADAMTS3, TRIM39, ADAMTS4, XDH, CYP1B1, AKAP13, MYO9A, ZFP451, RNF160, RNFT2, CASZ1, SLC31A2, SLC30A9, LOC100045359, DNMT3A, CRIP1, LPO, UPB1, NR4A2, SMG1, ZFP606, RIMKLA, CYP4B1, CDKN1A, RNF6, RNF150, ZFP773, PXDN, COPS5, ALOX12E, MLPH, RBM4B, ZCCHC8, CPXM2, 5730601F06RIK, GALNTL1, MBNL1, DMRTB1, ZFP652, RNF180, PPM1K, ZDHHC13, STEAP1, CYP51, ADAMTS19, CYP2F2, NR3C1, CPZ, ZFP317, TRIM11, TCEA3, FTHL17, RASGRP1, ZFP192, SLC39A8, USP33, SCO1, GALNT14, ZC3H12C, FADS1, ZFP386, TRIM25, ZFP2, ISL1, HBA-A1, HBA-A2, ZFP182, PHF16, ZMYND17
GO:0004601~peroxidase activity	4	0.06	4.56	0.87	LPO, PXDN, PRDX6, PRDX4

(continued)

Appendix Table 6. (continued)

GO:0016684~oxidoreductase activity, acting on peroxide as acceptor	4	0.06	4.56	0.87	LPO, PXDN, PRDX6, PRDX4
GO:0003712~transcription cofactor activity	11	0.06	1.95	0.85	KAT2B, COPS5, ATP6V0A1, TRIB3, SKI, MED13, RBM39, NRG1, CITED4, NRIP1, CITED2
GO:0005501~retinoid binding	3	0.06	7.37	0.85	RBP4, RBP7, RBP1
GO:0019840~isoprenoid binding	3	0.06	7.37	0.85	RBP4, RBP7, RBP1
GO:0030695~GTPase regulator activity	18	0.06	1.59	0.85	ARHGEF3, RALGPS2, MLPH, GPSM3, SIPA1L2, ARHGEF17, AKAP13, TRIO, DOCK8, DGKI, MYO9A, ARHGAP25, PLEKHG1, RASGRP1, KRIT1, ACAP2, TBC1D30, LOC100045359
GO:0003700~transcription factor activity	33	0.07	1.36	0.85	E2F2, MEF2A, E2F6, PRRX1, RORC, NFIX, NR3C1, CITED1, CITED2, MYCL1, POU5F2, ZFP192, HEY2, CREB3L4, RARB, POU3F1, PITX2, RHOX5, NR4A2, ARID3A, ZHX3, LEF1, SMAD3, TBX1, ISL1, DMRTB1, FOXN3, GCFC1, CSRNP2, IRF8, SPDEF, FOXC2, NFIC
GO:0008376~acetylgalactosaminyltransferase activity	4	0.07	4.26	0.83	CSGALNACT1, B4GALNT4, GALNTL1, GALNT14
GO:0005539~glycosaminoglycan binding	8	0.07	2.24	0.82	A930038C07RIK, EGFLAM, ADAMTS8, FGF9, PGLYRP1, APOH, PF4, VIT
GO:0019825~oxygen binding	3	0.07	6.84	0.82	HBA-A1, HBA-A2, CYP2F2, HBB-B1
GO:0060589~nucleoside-triphosphatase regulator activity	18	0.07	1.57	0.81	ARHGEF3, RALGPS2, MLPH, GPSM3, SIPA1L2, ARHGEF17, AKAP13, TRIO, DOCK8, DGKI, MYO9A, ARHGAP25, PLEKHG1, RASGRP1, KRIT1, ACAP2, TBC1D30, LOC100045359
GO:0004857~enzyme inhibitor activity	13	0.08	1.71	0.84	PHACTR1, TESC, C3, TRIB3, DGKI, SERPINI1, WFDC12, CDKN1A, BC048546, PPP1R1B, SERPINB12, EXPI, WFDC3
GO:0003697~single-stranded DNA binding	4	0.08	3.87	0.84	SSBP2, SSBP1, CSDA, HNRNPA1
GO:0043566~structure-specific DNA binding	6	0.09	2.52	0.85	SSBP2, SSBP1, FOXC2, SMAD3, CSDA, HNRNPA1
GO:0043125~ErbB-3 class receptor binding	2	0.09	21.29	0.84	NRG1, PIK3R1
GO:0003713~transcription coactivator activity	7	0.09	2.24	0.84	KAT2B, COPS5, ATP6V0A1, MED13, RBM39, CITED4, CITED2

KEGG Pathways	Up in E12.5 Bud Compared with E15 Bud				
Term	Count	*P*-value	Fold Enrichment	Q-value	Genes
mmu05200:Pathways in cancer	13	0.02	2.16	0.84	WNT10A, MAP2K1, FGF9, SMAD3, LEF1, ITGA3, FGF21, MMP2, VEGFC, LAMA1, CDKN1A, RARB, TCEB1
mmu05219:Bladder cancer	4	0.04	5.11	0.92	VEGFC, CDKN1A, MAP2K1, MMP2
mmu05412:Arrhythmogenic right ventricular cardiomyopathy (ARVC)	5	0.05	3.58	0.86	ITGA9, SGCG, LEF1, ITGA3, ITGA4
mmu00561:Glycerolipid metabolism	4	0.06	4.56	0.81	ALDH2, LCLAT1, DGKI, AGPAT4
mmu04512:ECM-receptor interaction	5	0.07	3.23	0.80	ITGA9, LAMA1, NPNT, ITGA3, ITGA4

(continued)

Appendix Table 6. (continued)

mmu04670:Leukocyte transendothelial migration	6	0.07	2.70	0.75	ICAM1, CLDN11, MSN, ITGA4, MMP2, JAM3
mmu00512:O-Glycan biosynthesis	3	0.09	5.96	0.79	GALNTL1, GCNT1, GALNT14
KEGG Pathways	Down in E12.5 Bud Compared with E15 Bud				
Term	Count	*P*-value	Fold Enrichment	Q-value	Genes
mmu04670:Leukocyte transendothelial migration	10	0.01	2.79	0.73	ICAM1, CLDN19, GNAI1, CLDN11, MSN, ITGA4, ITGB1, MMP2, JAM3, PIK3R1
mmu05219:Bladder cancer	5	0.04	3.95	0.93	E2F2, VEGFC, CDKN1A, MAP2K1, MMP2
mmu04512:ECM-receptor interaction	7	0.04	2.80	0.84	ITGA9, LAMA1, NPNT, ITGA3, ITGA4, ITGB1, THBS4
mmu04360:Axon guidance	9	0.04	2.28	0.78	PLXNA4, GNAI1, UNC5A, PLXNA2, SEMA4F, EFNB1, NTNG1, ITGB1, EPHB1
mmu04530:Tight junction	9	0.05	2.21	0.76	CLDN19, MAGI2, GNAI1, MPDZ, SPNB2, CLDN11, PPP2R2B, CSDA, JAM3
mmu00010:Glycolysis / Gluconeogenesis	6	0.05	2.93	0.72	ACSS1, ALDOC, FBP1, ALDH2, PFKP, ALDH3B1
mmu05200:Pathways in cancer	16	0.06	1.64	0.71	WNT10A, E2F2, MAP2K1, FGF9, SMAD3, LEF1, ITGA3, FGF21, ITGB1, MMP2, VEGFC, LAMA1, CDKN1A, RARB, TCEB1, PIK3R1
mmu05218:Melanoma	6	0.06	2.80	0.67	E2F2, CDKN1A, MAP2K1, FGF9, FGF21, PIK3R1
mmu04666:Fc gamma R-mediated phagocytosis	7	0.07	2.37	0.70	MAP2K1, LYN, WASF2, INPP5D, PIK3R1, AMPH, LOC100045359
mmu05412:Arrhythmogenic right ventricular cardiomyopathy (ARVC)	6	0.07	2.65	0.66	ITGA9, SGCG, LEF1, ITGA3, ITGA4, ITGB1

We generated the gene list by identifying genes whose expression differed 10-fold or higher between the E12.5 and E15 buds. This list was analyzed by DAVID (Database for Annotation, Visualization and Integrated Discovery) to identify overrepresented pathways and molecular function gene ontology terms. *P*-value for the group of genes was calculated by DAVID with a modified Fisher's Exact test (EASE-score). Fold enrichment was defined as the ratio of the percentage of the genes belonging to the pathway/term in the gene list analyzed compared with the percentage that would be expected by chance alone, and the Benjamini-Hochberg procedure was used to determine the false discovery rate (Q-value).

Appendix Table 7. Primer Sequences (Forward and Reverse) used for qPCR Validation of Microarray Data

Gene	Sense Primer	Anti-sense Primer
Mus musculus aquaporin 5 mRNA. **Aqp5**	GCCGTGGTGGTGGAGTTAATCTTG	CCAGTGTGACCGACAAGCCAATG
Mus musculus cadherin 1 mRNA. **Cdh1**	GACTAGGCTTATCTCAACCAAT	CCATCAAGAGCAGGCATT
Mus musculus cystic fibrosis transmembrane conductance regulator mRNA, complete cds. **Cftr** [a]	AGACCATCTAGCCTTACTACC	ACTAACACAACCTTCCTTCAC
Mus musculus catenin (cadherin associated protein), beta 1, transcript variant 1, mRNA. **Ctnnb1**[b]	GCGGTAGGGTAAATCAGTAAG	GCATCTGTTGAAGCATTGTATC
Mus musculus demilune cell and parotid protein 1 mRNA. **Dcpp1** [a b]	CCTTACTGATTCTTGCCTTCTT	CGTCCTTGTTGTCATCATAGT
Mus musculus demilune cell and parotid protein 2 mRNA. **Dcpp2**	CCTTACTGATTCTTGCCTTCTT	CCGTCCTCGTTGTCATTATAG
Mus musculus demilune cell and parotid protein 3 mRNA. **Dcpp3**	CCTTACTGATTCTTGCCTTCTT	AGTTGAGCCATACACTTGAC
Mus musculus dickkopf homolog 3 (*Xenopus laevis*) mRNA. **Dkk3**	ACCGCAGTAAGAGTGAGT	ATGTCTTGGAACAGAATGGATT
Mus musculus epidermal growth factor receptor mRNA, complete cds. **Egfr**	GAGTGCCAGACAAGACATC	CTCACAAGGTAGTGGACAATC
Mus musculus fibroblast growth factor receptor 2, transcript variant 2, mRNA. **Fgfr2** [a b]	GCATCATTCGGTTGAGAGT	TGTGAGGTGAGGTCTTGT
Mus musculus glycogen synthase kinase 3 beta mRNA. **GSK3**β	GTCACACTGCCGTCTCCACTCC	AGCTGCACCTCCTGTCTACACATC
Mus musculus integrin alpha 6, mRNA. **Itga6**	GTGCTAACAGAGTGGCTATC	CTATCCATTGGCAGTCTTGAG
Mus musculus potassium intermediate/small conductance calcium-activated channel, subfamily N, member 4, transcript variant 2, mRNA. **Kcnn4**	CACAGAAGAACCAGGCTAAG	GGAGGTCCAATTCAGTGTC
Mus musculus keratin 17 mRNA. **Krt17**	TCAGGATGGCAAGGTCAT	CACAGTTCACTTCAGGTCAG
Mus musculus keratin 18 mRNA. **Krt18**	GTTGTCACCACCAAGTCTG	TGTTCTCCAAGTTGATGTTCTG
Mus musculus keratin 7 mRNA. **Krt7**	CCTATTCCATCAAGACCACATC	AGCCAACAGCAGTTTCAG
Mus musculus keratin 8 mRNA. **Krt8**	GGCTGTGGTTGTGAAGAA	CACTTGGACACGACATCAG
Mus musculus laminin, beta 3 mRNA. **Lamb3**	GTCTCCACCATTGATAGCATAG	GGCACATTGTCCATTCCA
Mus musculus matrix metalloproteinase 2 mRNA. **Mmp2**	CCTTGGTGCTCCACTCTTCTGGTTCTTC	CAGTGCCCTCCTAAGCCAGTCTACTATTAAC
Mus musculus prolactin induced protein mRNA. **Pip**	ACAAACCCGCTGCCTCTGTAATG	GCCTCCGTTAATTCATTCGCACAG
Mus musculus sodium channel, nonvoltage-gated 1 alpha mRNA. **Scnn1a**	CTCCACCTGCCTATGCTA	GGAAGATGTGCTGAAGTGA
Mus musculus submandibular gland protein C mRNA. **Smgc**	TGCCACAGTCCAGGGTCAACAAG	CAGCCAGATTCCCACGGTCTCC
Mus musculus wingless-related MMTV integration site 10a mRNA. **Wnt10a**	AGGTGGTTGGCTCTTACA	AGATGACAGGAGGTAGGC
Mus musculus ribosomal protein S29 mRNA. **RPS29** [c]	ATGGGTCACCAGCAGCTCTACTG	GGAAGCACTGGCGGCACATG
Mus musculus wingless-related MMTV integration site 6 mRNA. **Wnt6** [b]	GTCTATCATTCCACCTGTTACC	GACGCCTGACAACTAAGC

Key: a - used for validating E12.5 duct *vs*. E15 main duct expression; b - used for validating E12.5 bud *vs*. E12.5 main duct expression; c - gene used to normalize expression. The bolded text in column 1 is the gene symbol.

Appendix Table 8. Differential Gene Expression between Locations Identified by ANOVA

E12.5 Arrays (25378 genes present, 3841 pass through ANOVA)

	Bud	Cleft
Bud	–	682
Main duct	2028	2519

E13.5 Arrays (22067 genes present, 3698 pass through ANOVA)

	Central Bud	Secondary Duct	Main Duct	Cleft
Central bud	–	255	1889	241
Peripheral bud	34	752	2340	104
Cleft	241	473	1768	–
Secondary duct	255	–	357	473

E14 Arrays (18613 genes present, 2283 pass through ANOVA)

	Bud	Secondary Duct
Bud	–	912
Main duct	1275	807

E15 Arrays (17656 genes present, 5313 pass through ANOVA)

	Bud	Secondary Duct
Bud	–	2358
Main duct	3247	1860

Numbers at intersections show number of genes expressed differently between the 2 locations as identified by Tukey's *post hoc* test.